Characterization of Fatigue Damage in Composite Sandwich Hull Materials at Low Temperatures

Samirkumar M. Soni, Ronald F. Gibson, Emmanuel O. Ayorinde

Mechanical Engineering Department
Advanced Composites Research Laboratory
Wayne State University
Detroit, MI 48202 USA

Keywords*: Composite sandwich; foam core; low temperature; fatigue*

Abstract

This paper summarizes the results of experimental and numerical studies on the fatigue behavior of foam core carbon/epoxy composite sandwich (CS) beams at room temperature (RT) and low temperatures (down to -60 ^{0}C) for their potential applicability in the hull materials of ships navigating in the Polar Regions. 4-point static flexural test results confirmed the clear effects of low temperatures on the stiffness, strength, elastic limit and brittleness of the CS beams. Core shear was found to be the dominant failure mode under fatigue loading conditions at -60 ^{0}C. Significant increases in the useful fatigue life with brittle type core shear failure were observed at low temperatures by comparison with the corresponding RT behavior. Two approaches were used to investigate stiffness reductions during useful fatigue life. The static finite element analysis (FEA) explained the effects of skin stiffness on the crack initiation location under fatigue loading conditions.

1 Introduction

Nowadays foam core sandwich structures are widely used in boat and ship hull structures. The low weight to strength ratio and relative ease in producing large composite sandwich components; and even the possibility of constructing the entire hull as an entity make composite sandwich structures attractive for such applications [1, 2]. In these applications, the structure is constantly battered by waves, which means that fatigue is of concern. Under such long-term cyclic loading conditions, failure mechanisms in the sandwich composite structures may be more complex than those of metal or ceramic counterparts. Moreover, the fatigue life of composite sandwich structures is influenced by various factors. Specifically, ships navigating around the Polar Regions, where atmospheric temperatures remain below 0 ^{0}C with frozen sea surface throughout the year, also experience the severe effects of such low temperatures on the ship hull structure. Generally, polymeric composites exhibit higher strength and stiffness but reduced ductility at low temperatures. Thus, the failure modes of composite sandwich structures under cyclic loading at low temperatures (below freezing point temperatures) may change and therefore a thorough study of the fatigue behavior of composite sandwich structures at low temperatures is of great importance.

A significant amount of research has been published explaining the static and fatigue behavior of composite sandwich structures [3]. Daniel, et al [4], and Steeves and Fleck [5, 6] studied in detail the failure mechanisms in foam core sandwich beams under static loading and observed four different modes of failure: (1) core shear (2) face sheet wrinkling (3) face sheet micro buckling and (4) face sheet indentation. Harte et al. [7] examined failure modes in aluminum foam core sandwich beam under both static and fatigue loading conditions. Burman and Zenkert [8, 9] studied fatigue characteristics of foam core sandwich beams experimentally as well as analytically. Based on these extensive experimental results, it was concluded that the predominant failure mode under cyclic fatigue was core shear. This is due to the fact that the cyclic loading appears to reduce the residual shear strength of the foam core. Kanny and Mahfuz [10] showed that the stiffness and fatigue strength of sandwich beams increased with increased core density and the number of cycles to failure increased with the frequency but the time to failure showed the opposite trend. This seems to contradict statements by Burman and Zenkert [8, 9] and by Sharma, et al. [11] that increasing frequency has detrimental effects on the fatigue life in terms of number of cycles to failure due to the corresponding increase in core temperature.

Berkowitz and Johnson [12] found that the fracture toughness of composite sandwich structures comprised of a Nomex honeycomb core with graphite/epoxy skins increased with corresponding reduction in temperature and the cold temperatures resulted in slower fatigue crack growth rates than at room temperature, while hot temperatures caused faster fatigue crack growth rate in the core. Kanny, et al. [13] specifically investigated the effects of elevated temperatures (up to 80^0 C) on the fatigue behavior of foam core sandwich structures. However, it appears that no work has been published so far showing the effects of low temperatures on the fatigue life and failure modes of foam core composite sandwich beams.

The present work describes the characterization of the effects of low temperatures on low cycle flexural fatigue behavior of unidirectional carbon fiber/Rohacell foam core (CF/RC) sandwich beams by using experimental and FEA methods. The main aim of the study is to determine the effects of low temperature on the failure modes under static and fatigue loading conditions and on the fatigue life of the composite sandwich beams.

2 Experiments

2.1 Materials and specimens

In this study, T300/A534 carbon fiber/epoxy sandwich constructions with closed cell PMI (polymethacrylimide) rigid foam (Rohacell 71 IG (Industrial Grade)) cores were used. The carbon fiber/epoxy face sheets (thickness = 0.028 inch) have 3 layers of unidirectional laminae with fiber direction along the length of the beam. All the specimens were 8 inches long with (1 in X 0.556 in) cross sectional dimensions. The foam was 100% closed cell, homogeneous and isotropic.

2.2 Static 4-point bending tests

It was necessary to first benchmark the static flexural strength and stiffness of the specimens at RT and different low temperatures before performing the fatigue tests. Since the literature survey indicated that core shear is the dominant mode of failure under flexural fatigue loading conditions, static 4-point bending tests were performed on the CS beams in accordance with the ASTM standard C 393-00 [14] to check for possible core shear failure under static loading.

Static 4-point bending tests were performed on the CF/RC sandwich beams at 22 ^{0}C, 0 ^{0}C, -30 ^{0}C and at -60 ^{0}C respectively inside the environmental chamber of an EnduraTec servo-pneumatic testing machine (Fig. 1) in order to establish a baseline on static behavior at different temperatures. Three replicate specimens of the CS beams were used for the static tests at each temperature.

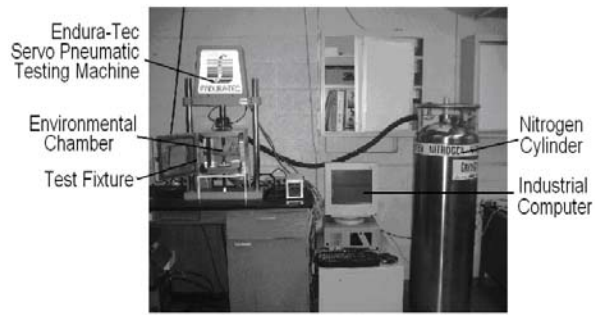

Fig. 1. Test set up for 4-point bending tests.

The loading configuration was quarter point loading with a 4.72 inch span and 1.57 inches between the loading points. The support and loading pins each had a diameter of 0.315 inches to avoid local face sheet indentation failure. The experiments were performed under displacement-control at a crosshead speed of 0.0002 inch/sec until failure. The loading rate and the response of the system were controlled and recorded with the help of the Endura-Tec Win-Test software. A digital camera and StreamPix software on a personal computer were used to monitor and record the failure events during the test with a scanning rate of 11 frames per second (fps). The temperature of the hot-cold chamber was controlled by the EnduraTec Win-Test software through a PC 200 temperature controller. Evaporated liquid nitrogen was used as the coolant.

2.3 Flexural fatigue tests

4-point flexural fatigue tests were performed on CF/RC beams in accordance with ASTM C-393-00 [14] under load control at RT, 0 ^{0}C and at -60 ^{0}C at 2 Hz and different load levels to investigate the changes in the low cycle fatigue behavior of the CF/RC sandwich beams at low temperatures. The same type of test set up was used for fatigue tests as for the static 4-point bending tests (Fig. 1). By using the ultimate strength data acquired from the static 4-point bending tests at different temperatures, the maximum flexural load applied per cycle was determined at different load levels, r, as defined by:

$$r = \frac{P_{max}}{P_{ul}} \qquad (1)$$

Where P_{max} is the maximum load applied per fatigue cycle and P_{ul} is the ultimate failure load applied during static loading. The minimum flexural load applied per cycle was determined from the loading ratio R, as defined by:

$$R = \frac{P_{min}}{P_{max}} \qquad (2)$$

Where P_{min} is the minimum flexural load applied per cycle. The loading ratio, R = 0.1 was kept constant during all the fatigue tests to observe the sole effect of low temperature on the fatigue behavior. Initially, flexural fatigue tests were performed at room temperature, different load levels (from r = 0.9 to r = 0.6) and a frequency of 2 Hz on CF/RC sandwich beams. The maximum test running time at any load level was 48 hrs (3,45,600 cycles) by considering the unforeseen fatigue behavior of CF/RC beams at low temperatures and limited availability of liquid nitrogen per cylinder. Three replicate specimens of the CS beams were used for the fatigue tests at each temperature.

Fatigue data was acquired and saved in two different ways during each fatigue test. In the first type of data acquisition file, 25 points were scanned and stored per fatigue cycle showing load applied at specific points during each fatigue cycle as well as the system response in terms of displacement of crosshead in the vertical direction at those points. These data points were used to plot the hysteresis loops of applied load vs. crosshead displacement in a particular fatigue loading cycle. The hysteresis loops were then analyzed to determine the stiffness and damping factors during that cycle.

In the second type of data acquisition file, only peak-valley points for each fatigue loading cycle and the corresponding crosshead displacements were stored in order to determine the stiffness reduction associated with that particular number of cycles.

3 Finite Element Analysis (FEA)

In order to better understand the stress distributions, the corresponding failure points, and the effects of differences in coefficients of thermal expansion between skin and core on the failure mode, FEA was performed. A 2D FEA model of an undamaged CF/RC beam, which was created by Baba. et al. [15], was employed. Moreover, to predict the behavior of both types of beams at low temperatures, an approximate coefficient of thermal expansion for each component was added in the model. For the static FEA, HyperMesh 7.0 was used as pre-post processor and ABAQUS 6.5 was used as a solver The CF/RC beam model was subjected to three types of loading: 1) mechanical four point bending loading at room temperature, 2) thermal loading by decreasing the temperature of the model from RT to -60 ^{0}C, and 3) both thermal and mechanical loading by applying the mechanical four point bending loading load at -60 ^{0}C.

4 Results and Discussion

4.1 Static 4-point bending tests

Static four point bending tests were performed at 22 ^{0}C, 0 ^{0}C, -30 ^{0}C and at -60 ^{0}C to benchmark the strength of the CF/RC sandwich beams at the respective temperatures. For each case, during the loading period no cracks were visually observed through the digital camera up to the final failure point. All specimens failed suddenly due to core shear at all of the temperatures, as seen in Fig. 2.

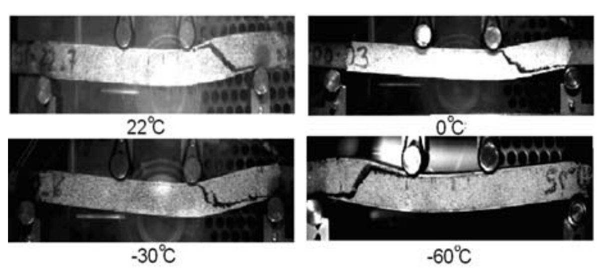

Fig. 2. Modes of failure of carbon fiber/Rohacell foam sandwich beams at different temperatures.

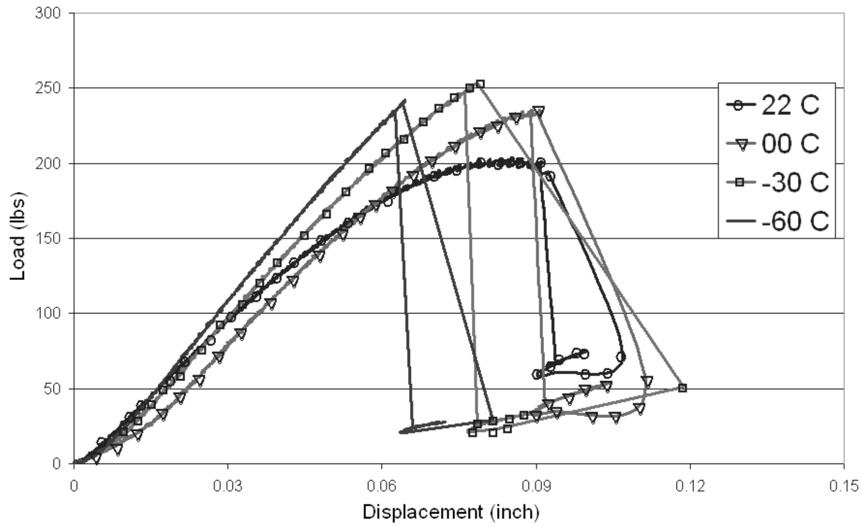

Fig. 3. Load – crosshead displacement graphs for CF/RC beams under static flexural loading conditions at different temperatures.

The entire crack formation and growth sequence occurred in a fraction of a second, so it was not possible to follow the sequence exactly with the digital camera. However, the final crack pattern observed under static loading appeared to be quite similar to that reported in the literature for fatigue loading. The effects of temperature on the stiffness, strength and ductility of the sandwich beams are clearly shown in the load-displacement curves in Fig. 3. The CF/RC sandwich beams exhibited increased stiffness with corresponding reductions in the temperature. The slope, elastic limit and displacement at failure all varied almost linearly with respect to temperature change. At room temperature, the CF/RC beams exhibited significant yielding and ductile behavior, but a more brittle type sudden failure occurred near the ultimate loading points at -30 ^{0}C and at -60 ^{0}C, with corresponding reductions in the displacement at failure.

The average ultimate flexural strength of the CF/RC beams increased with corresponding reductions in temperature. However, the jump in ultimate strength data is more prominent during temperature reduction from 22 ^{0}C to 0 ^{0}C than during 0 ^{0}C to -60 ^{0}C. The corresponding displacement at failure for all specimens decreased with reductions in temperature.

4.2 Flexural fatigue tests

The main purpose of the fatigue tests on the CF/RC beams was to compare the fatigue life, fatigue failure mode, stiffness and damping factors at low temperatures with the corresponding RT behavior. The experimental results of flexural fatigue tests performed on CF/RC beams at different load levels, r, and different temperatures are presented in Table 1 in terms of number of cycles to failure, N_f , where N_f was recorded just before final failure.

4.2.1 Fatigue life at low temperatures

The fatigue life data of CF/RC sandwich beams at different load levels and temperatures were presented by using modified S-N curves. For convenience, the modified S-N curves were plotted with maximum applied load /ultimate load, P_{max}/P_{ul}, (which is also defined as the load level, r) on the Y-axis, and the logarithm of the number of cycles to failure on the X- axis. The modified S-N curve data at different temperatures are shown in Fig. 4. At all temperatures, the specimens exhibited increases in the number of cycles to failure with reductions in the load level, r. The rate of increase in N_f with reductions in load level consistently increases with reductions in temperature, and the fatigue life at a temperature of –60^{0}C is nearly one hundred times greater than the fatigue life at RT.

Table 1. Fatigue life data of CF/RC beams at different load level and temperatures.

Load level (r)	Temperature					
	22 ^{0}C		0 ^{0}C		- 60 ^{0}C	
	load Applied (lb)	Avg. No. of Cycles to failure	Load Applied (lb)	Avg. No. of Cycles to failure	Load Applied (lb)	Avg. No. of Cycles to failure
1 (static)	**201**	**0.25**	**230**	**0.25**	**235**	**0.25**
0.9	**180**	**258**	**207**	**528**	**210**	**24872**
0.85	**170.8**	**290**	**195.5**	**650**	**199.75**	**33146**
0.7	**140.7**	**3328**	**161**	**5580**	**-**	**-**
0.6	**120.6**	**49622**	**-**	**-**	**-**	**-**

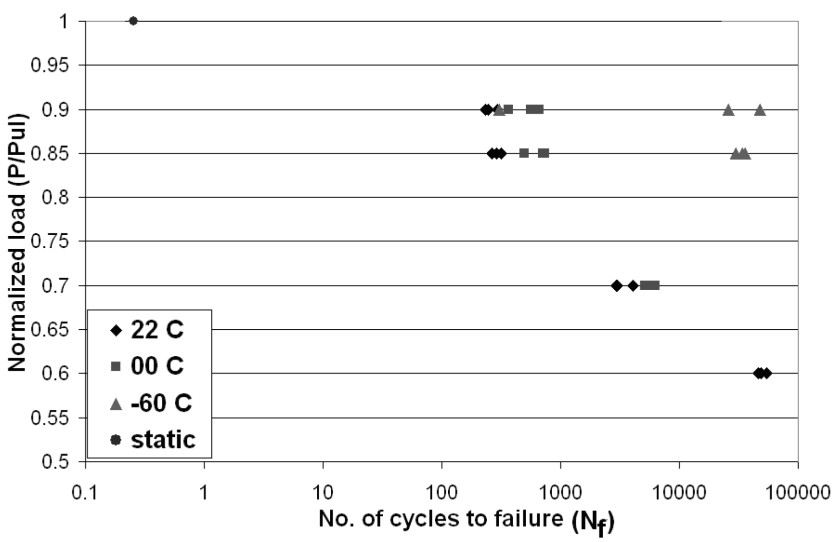

Fig. 4. Modified S-N curve data for CF/RC sandwich beams showing effect of low temperatures on fatigue life at different load levels.

The increment in the flexural fatigue life at -60 ^{0}C was consistent for CF/RC beams at 0.90 and 0.85 load levels. Thus, it was clear that the fatigue life of composite sandwich beams would be much improved at low levels of loading at -60 ^{0}C.

4.2.2 Effects of low temperature on stiffness and damping ratio

Two approaches were used to determine the stiffness reduction during flexural fatigue tests performed on CF/RC beams at different load levels and temperatures. In the first approach, graphs were plotted for CF/RC beams using the absolute mean crosshead displacement (Fig. 5) per cycle as ordinate and number of cycles as abscissa as shown

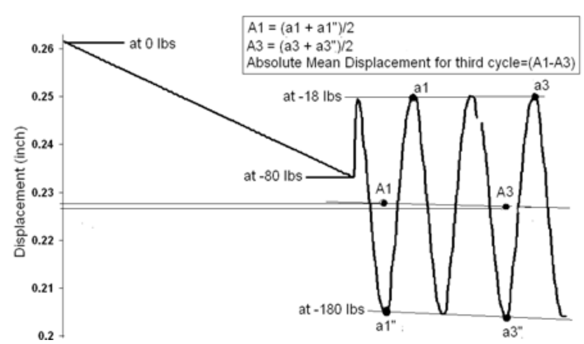

Fig. 5. Calculation of absolute mean displacement for each cycle.

in Fig. 6. For each graph, the final data points show the deformation of the beam just before the core shear failure. The final core shear stage is not included in these graphs. These graphs provide important information about the stiffness reduction during the fatigue tests, as each fatigue test was performed under load control and so changes in the absolute mean displacement with increasing number of cycles indirectly provide a measure of stiffness reduction during that period.

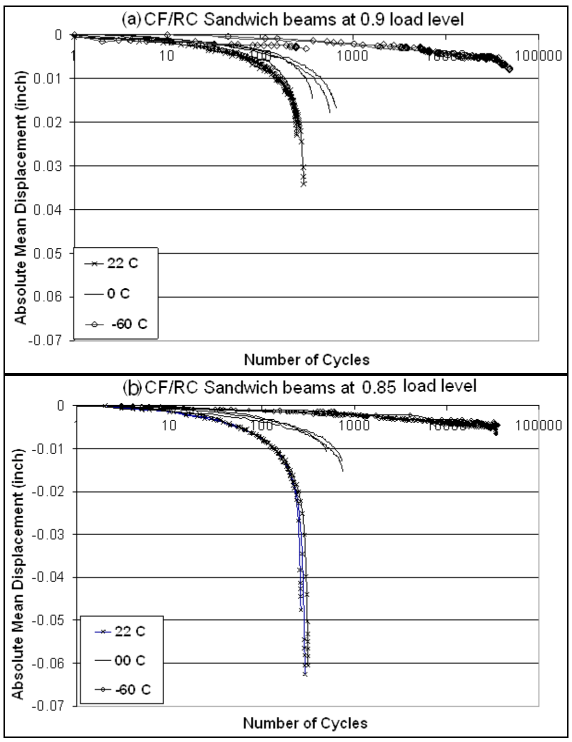

Fig. 6. Absolute mean displacement vs. number of cycles for CF/RC beams at 0.9 (a) and 0.85 (b) load levels and different temperatures.

General observations from Fig. 6 are: (1) there was a clear effect of temperature reduction on the stiffness degradation during fatigue testing. At RT, the stiffness reductions gave early warning of impending fatigue failure, well in advance of the failure, (2) At 0 ^{0}C, the slope of the absolute mean displacement curves decreased by comparison to those at RT for each load level, but there was still enough of a change in the slopes of the curves to give some early warning, (3) At -60 ^{0}C, the total absolute mean displacement was very low up to the failure point with negligible early warning compared with the RT data, and there was no sign of impending failure throughout the duration of the fatigue tests, (4) the specimens became stiffer and stronger against fatigue loading at low temperatures and exhibited tremendous increases in fatigue life but with catastrophic fatigue failure and little early warning, (5) the number of cycles to failure was shifted for CF/RC beams with reduction in temperature, at both 0.9 and 0.85 load levels, but after a certain deformation (absolute mean displacement = 0.004 to 0.005 inch), the curves exhibited nonlinearity irrespective of temperature. At RT and at 0 ^{0}C, the specimens were ductile and exhibited plastic-like deformation by exhibiting slow increases in core shear crack growth rate, but at -60 ^{0}C as they became brittle and failed suddenly during the shift from the elastic to the plastic deformation region.

In the second approach, dynamic stiffness, S, and loss factor, LF, of the specimens were determined from the hysteresis loops at specific numbers of cycles during the fatigue life at 0.9 and 0.85 load levels and at RT, 0 ^{0}C and -60 ^{0}C as shown in Fig. 7, where [16],

$$S = (a/2) / (b/2) \quad (3)$$
$$LF = (c/2) / (a/2) \quad (4)$$

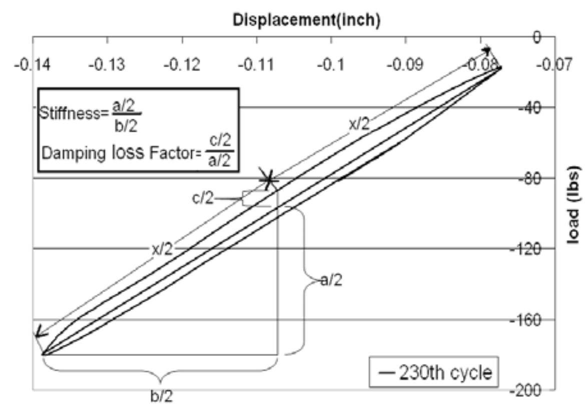

Fig. 7. Hysteresis loop for determination of stiffness and damping loss factor.

These equations were based on the assumption of a perfectly elliptical hysteresis loop for each fatigue cycle. These representative points showing stiffness and damping factors at different number of cycles were plotted on different graphs respectively as shown in Fig. 8. The following observations were made from the graphs in Fig. 8:

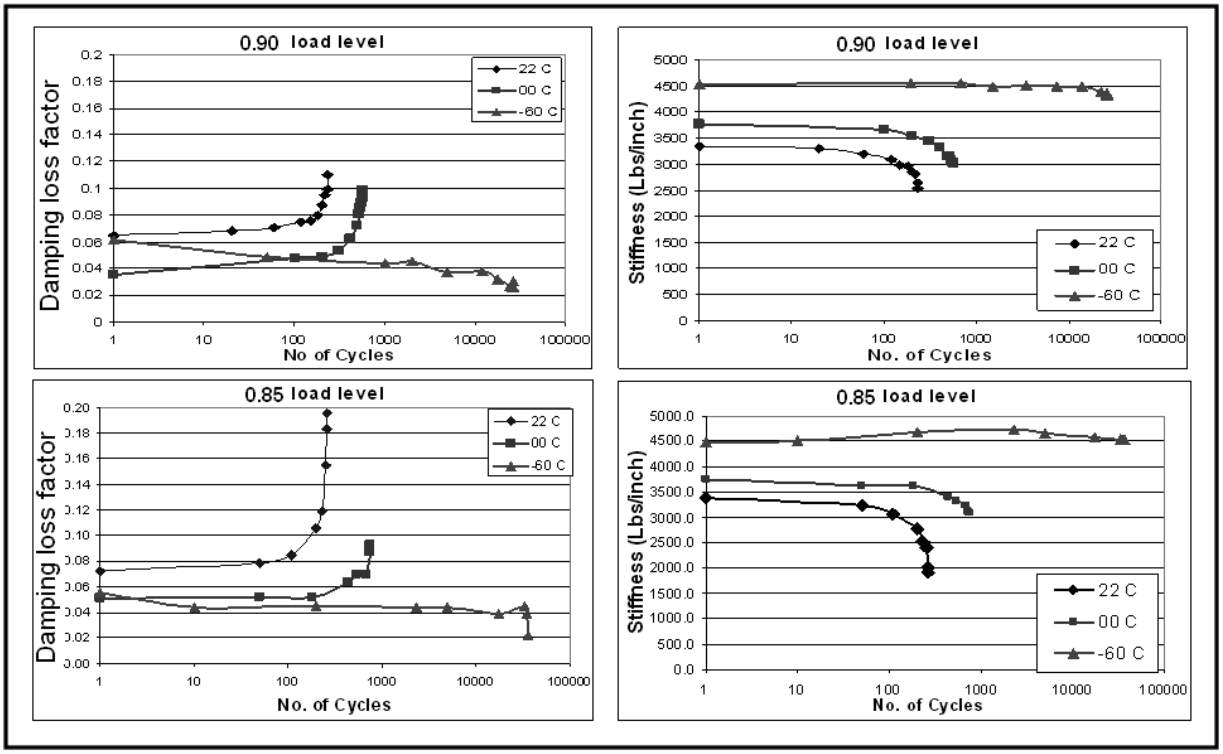

Fig. 8. Graphs showing changes in stiffness and damping loss factors of CF/RC beams during fatigue loading at different temperatures and load levels.

(1) A definite increase in the initial stiffness is noticeable at the start of the fatigue tests with reduction in the temperature, while the damping loss factors showed negligible initial difference, (2) at RT, the stiffness curves sloped downwards while damping loss factor curves sloped upwards with increasing numbers of cycles at both 0.9 and 0.85 load level. Both curves exhibited significant nonlinearity leading to final failure, (3) at 0 ^{0}C, both stiffness and damping factor curves exhibited behavior similar to that at RT, but the amount of nonlinearity in the curves was reduced at both load levels, (4) at -60 ^{0}C, the stiffness curves were almost flat throughout the fatigue life at both 0.9 and 0.85 load levels with little nonlinearity in the last few cycles. So at -60 ^{0}C, the effect of fatigue loading on the stiffness was negligible and that was the reason behind much longer fatigue life, (5) the damping factor curve sloped downwards a bit with increasing numbers of cycles at -60 ^{0}C and at both load levels.

4.2.3 Modes of failure under fatigue loading conditions

A digital camera and StreamPix software were used to monitor the failure modes and crack progression throughout the fatigue tests and Fig. 9 explains the observed fatigue failure sequence. Small shear cracks were generated inside the core in the region between the loading point and the supporting point after 90 to 95% of the useful fatigue life at RT and 0 ^{0}C. The stiff unidirectional carbon fiber/epoxy skin did not allow any skin indentation and local crushing of the core below the loading point or above the supporting point. Thus, small shear cracks were generated in the region between the loading point and the supporting point, where maximum shearing stresses were generated under flexural cyclic loading.

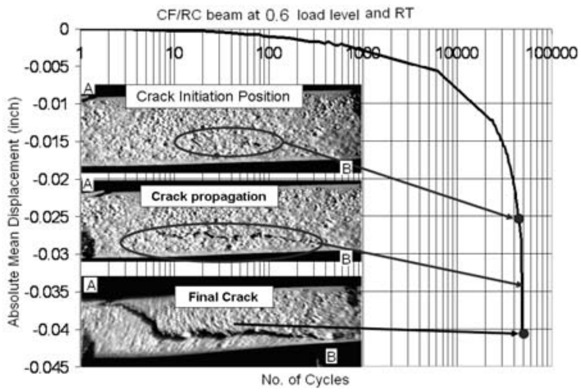

Fig. 9. Core shear failure sequence in CF/RC beam under flexural fatigue loading.

These small cracks coalesced and formed a single leading crack with increasing numbers of cycles. Then the crack shot suddenly towards both compression and tension side skin-core interfaces producing the final failure event as shown in Fig. 9. At -60 ^{0}C, the CF/RC beam failed with the same sequence but again the whole failure event took place in the final few cycles..

4.3 Finite element analysis (FEA) results

FEA was performed to predict the behavior of composite sandwich beams. Fig. 10 shows comparisons of the predicted load–displacement curves from static FEA with the experimental static 4-point bending test results for the sandwich beams.

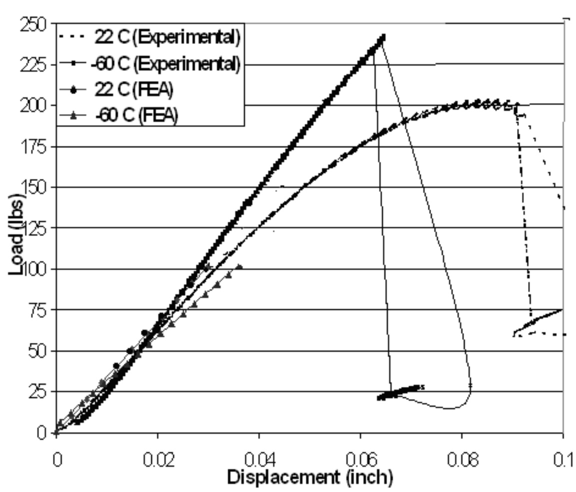

Fig. 10. Comparison of static load-displacement curves obtained from experiments and FEA for CF/RC beams.

At RT, the slope of the linear elastic region of the curves obtained from FEA matched well with the experimental values of slope. However, there were little or no apparent thermal effects on the results at -60 ^{0}C for the FEA model, because data on the temperature dependence of skin and core properties were not available. Thus, the present models were only useful for predicting the behavior of sandwich beams at RT.

In another analysis on the same model, the von Mises stress contours generated inside the core along the length of the beam were investigated for the CF/RC beam subjected to static load only as shown in Fig. 11.

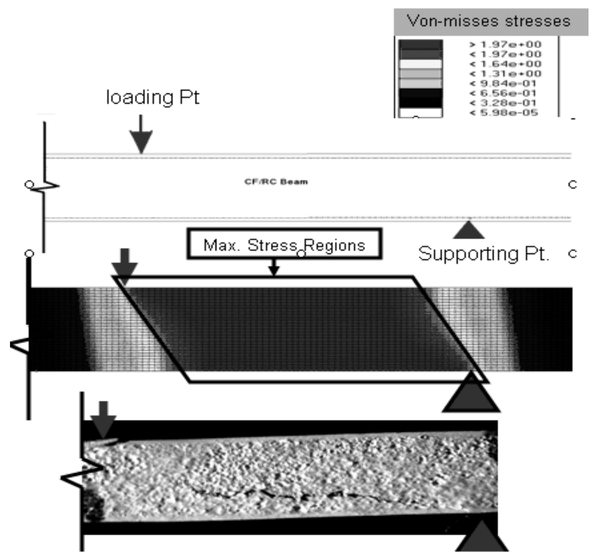

Fig. 11. von Mises stress contours from the FEA .

The static load applied was 100 lbs, which was well below the elastic limit of the CF/RC beam. The results showed that the von Mises stresses were almost uniformly distributed along the region in-between the loading points and the supporting points. The reason behind this was that the high stiffness of the unidirectional carbon/epoxy skin did not allow skin indentation and core crushing near the loading point and supporting point areas. Thus, these predictions from the static FEA threw more light on the experimentally observed failure initiation phenomena of CF/RC beams. The failure started with minute shear cracks in the region between the loading points and the supporting points.

5 Conclusions

The effects of low temperature on the flexural fatigue behavior and the fatigue crack propagation rates of CF/RC sandwich composites have been investigated and the following conclusions have been drawn from this study:

(1) specimens failed with sudden core shear failure under the four point static loading conditions at each temperature (22 ^{0}C, 0 ^{0}C, -30 ^{0}C and -60 ^{0}C). From the increases in the slopes of the load – displacement curves and the elastic limit and the corresponding decrease in the displacement at failure with temperature reduction, it is clear that the stiffness as well as brittleness increases for the CF/RC beams with corresponding temperature reductions.

(2) core shear was the only failure mode observed under the flexural static loading conditions at different temperatures and there was no effect of low temperature on the failure mode of the sandwich beams.

(3) at 0 ^{0}C, specimens failed after more than twice the number of cycles than at RT but at -60 ^{0}C and high load levels, the fatigue lives were increased by almost hundred times compared with the RT values. The reason behind this is believed to be the increase in the stiffnesses of both skin and core materials at low temperatures.

(4) the stiffness reductions during the fatigue tests were measured by two different methods which gave results that were in good agreement.

(5) At 0 ^{0}C, the amount of warning and the slope of the absolute mean displacement vs. number of cycles was decreased, which was a clear indication of failure transition from ductile type to brittle type behavior. At room temperature and at 0 ^{0}C, specimens showed significant failure warnings by the increase in the rate of stiffness reduction and the appearance of minute visible cracks during fatigue loading after almost 85 % of the useful life.

(6) At -60 ^{0}C, CF/RC beams became extremely stiff and exhibited very little reduction in stiffness during the whole fatigue life. In addition, there was a significant increase in the fatigue life with sudden brittle type core shear failure without any failure warning in the form of minute cracks or stiffness reduction. Thus, for low temperature working conditions, it is difficult to monitor failure events in these structures and to take any safety measures.

(7) it was confirmed from the FEA that the unidirectional carbon/epoxy skin was stiff enough so the core shear cracks start somewhere in the core instead of starting just below the loading point due to core crushing.

6 Acknowledgements

The authors gratefully acknowledge the financial support of the U. S. Office of Naval Research, and the guidance of ONR Program Officers Dr. Kelly Cooper and Dr. Yapa Rajapakse.

7 References

[1] Allen H.G. "*Analysis and design of structural sandwich panels*". Paragon Press, London, 1969.

[2] Vinson J. R. "*The Behavior of Sandwich Structures of Isotropic and Composite Materials*". Technomic Pub. Co., Lancaster, PA, 1999.

[3] Sharma N., Gibson R. F. and Ayorinde, E. O. "Fatigue of Foam and Honeycomb Core Composite Sandwich Structures: A Tutorial", *Journal of Sandwich Structures and Materials*, Vol. 8, No. 4, pp 263-319, 2006.

[4] Daniel I. M. Gdoutos E. E., Wang K. A. and Abbot J. L. "Failure modes of composite sandwich beams", *International Journal of Damage Mechanics*, Vol. 11, pp 309-334, 2002.

[5] Steeves C. A. and Fleck N. A. "Collapse mechanisms of sandwich beams with composite faces and a foam core, loaded in three-point bending. Part I: analytical models and minimum weight design", *International Journal of Mechanical Sciences*, Vol. 46, pp 561-583, 2004.

[6] Steeves C. A. and Fleck N. A. "Collapse mechanisms of sandwich beams with composite faces and a foam core, loaded in three-point bending. Part II: experimental investigation and numerical modeling", *International Journal of Mechanical Sciences*, Vol. 46, pp 585-608, 2004.

[7] Harte A. M. Fleck N. A. and Ashby M.F. "The fatigue strength of sandwich beams with an aluminum alloy foam core", *International Journal of Fatigue*, Vol. 23, pp 499-507, 2001.

[8] Burman M. and Zenkert D. "Fatigue of foam core sandwich beams – 1: undamaged specimens", *International Journal of Fatigue*, Vol. 19, No. 7, pp 551-561, 1997.

[9] Burman M. and Zenkert D. "Fatigue of foam core sandwich beams – 2: effect of initial damage", *International Journal of Fatigue*, Vol. 19, No. 7, pp 563-578, 1997.

[10] Kanny K. and Mahfuz H. "Flexural fatigue characteristics of sandwich structures at different

loading frequencies", *Composite Structures*, Vol. 67, pp 403-410, 2005.

[11] Sharma S.C., Murthy H.N.N. and Krishna M. "Interfacial studies in fatigue behavior of polyurethane sandwich structures", *Journal of Reinforced Plastics and Composites*, Vol. 23, No. 8, pp 893-903, 2004.

[12] Berkowitz C. K. and Johnson W. S. "Fracture and fatigue tests and analysis of composite sandwich structure", *Journal of Composite Materials*, Vol. 39, No. 16, pp 1417- 1431, 2005.

[13] Kanny K., Mahfuz H., Thomas T. and Jeelani S. "Temperature effects on the fatigue behavior of foam core sandwich structures", *Polymers and Polymer Composites*, Vol. 12, No. 7, pp 551-559, 2004.

[14] *Annual Book of the ASTM Standards*. C 393-00: Standard Method of Flexure Test of Flat Sandwich Constructions, American Society for Testing and Materials, Philadelphia, PA. Vol. 15. No. 03, pp 23-24, 2000.

[15] Baba B. O., Gibson R. F. and Soni, S.. "The Influence of Fatigue Cracks on the Modal Vibration Response of Composite Sandwich Beams", *Proc. 21st Annual Technical Conference of the American Society for Composites*, Dearborn, Michigan, Sept. 17-20, paper no. 101, 2006.

[16] Gibson R. F., "*Principles of Composite Material Mechanics*". McGraw-Hill, New York, 1994.